

Rotating oil droplets driven by motile bacteria at interfaces

Narendra K. Dewangan and Jacinta C. Conrad*

Department of Chemical and Biomolecular Engineering, University of Houston, Houston, TX 77204-4004

*Email: jconrad@uh.edu

Number of pages: 6

Number of figures: 11

Number of tables: 3

Number of movies: 4

1 Supplementary movies

S1.avi : Counter-clockwise rotation of 55 μm dodecane droplet near the bottom surface of microcapillary channel. The cell concentration was 2.7×10^8 cells mL^{-1} .

S2.avi : Clockwise rotation of 48 μm dodecane droplet near the top surface of microcapillary channel. The cell concentration was 2.7×10^8 cells mL^{-1} .

S3.avi : Rotation behavior of dodecane droplet at 1000 ppm DOSS concentration at cell concentration of 2.7×10^9 cells mL^{-1} .

S4.avi : Dodecane droplets do not rotate at 3500 ppm DOSS concentration at cell concentration of 2.7×10^9 cells mL^{-1} . A random motion of particles (non-adhering) are seen on droplets.

2 Surface properties of bacteria

Table S1 Zeta potential of PS particles and different bacteria strains used in this study. Standard deviations are calculated based on three different samples.

Sample	Mobility [m.u.]	Zeta potential [mV]
Sulfate-modified PS particles	-3.0 ± 0.1	-39 ± 2
<i>Halomonas titanicae</i>	-3.6 ± 0.3	-46 ± 3
<i>Shewanella haliotis</i>	-2.7 ± 0.4	-34 ± 5
<i>Escherichia coli</i> MC1061	-3.0 ± 0.1	-39 ± 2

Table S2 Contact angle and surface energy of bacteria. Standard deviations are calculated based on at least two bacteria lawns. The surface energy of bacteria lawn is calculated from method of Wu.^{1,2}

Bacteria species	Water [°]	DIM [°]	EG [°]	Surface energy [mN m^{-1}]
<i>Halomonas titanicae</i>	23 ± 4	57 ± 5	29 ± 4	64 ± 1
<i>Shewanella haliotis</i>	14 ± 2	45 ± 4	26 ± 4	66 ± 1
<i>Escherichia coli</i> MC1061	19 ± 2	60 ± 6	17 ± 2	66 ± 1

Table S3 Oil-water interfacial tension. Water contains 10 gL^{-1} of potassium nitrate.

Oil phase	Aqueous phase	Interfacial tension [mN m^{-1}]
dodecane	water	46 ± 1
hexadecane	water	51 ± 1

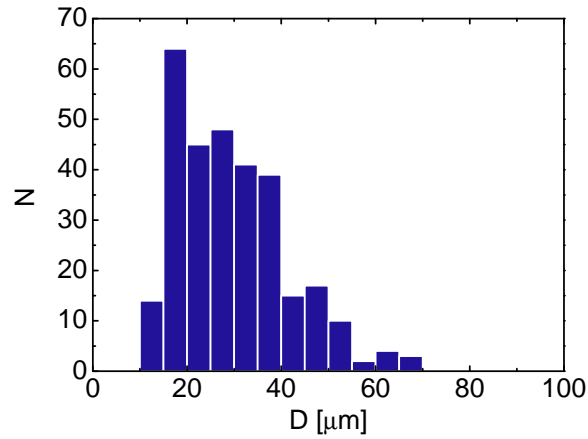


Fig. S1 Distribution of the diameter of dodecane droplets prepared by shaking 20 μL of dodecane in 500 μL of water ($10 \text{ g L}^{-1} \text{ KNO}_3$). The sample was introduced into an imaging chamber immediately after because droplets were not stable without added surfactant.

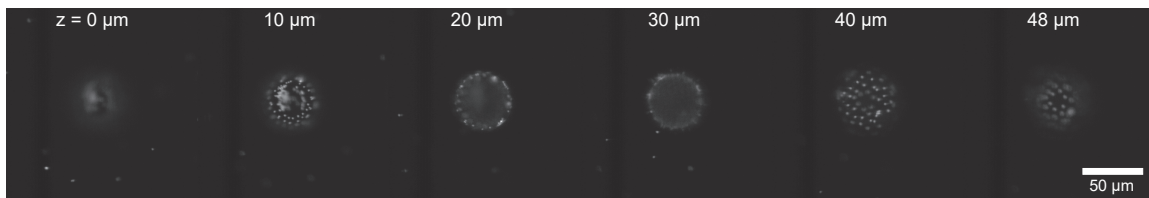


Fig. S2 Micrograph of polystyrene (PS) particles attached to the dodecane-water interface. The label in each panel indicates the distance of focal plane from the bottom surface of the droplet. The outer aqueous phase is 10 g L^{-1} potassium nitrate in water.

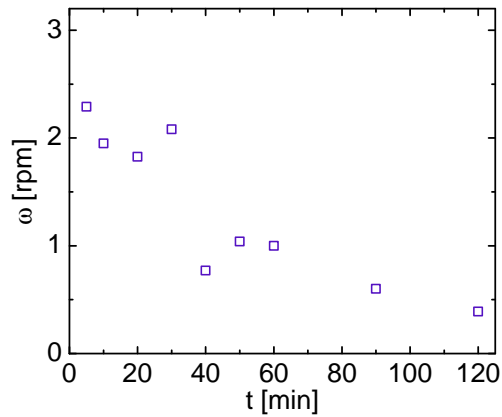


Fig. S3 Angular speed of a 40 μm dodecane droplet as a function of time. The droplet rotated for more than 2 h, but its angular speed decreased markedly after 30 min. The angular speed was measured for the same droplet over time and each point of the plot is for one droplet. The optical density of cells suspension was 1.0 ($2.7 \times 10^9 \text{ cells mL}^{-1}$). The aqueous phase is water (10 g L^{-1} potassium nitrate) without added surfactant.

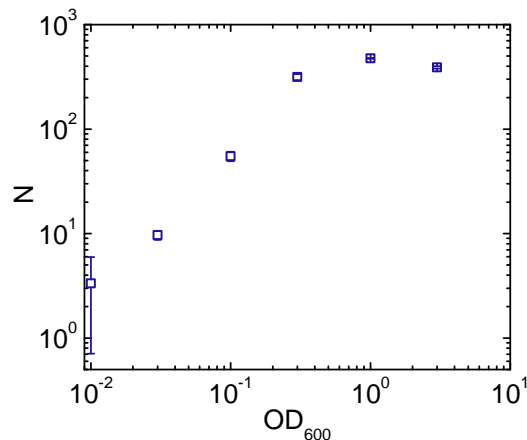


Fig. S4 Number of cells (*H. titanicae*) adhered on 40 μm dodecane droplets as a function of optical density. The aqueous phase is water (10 gL^{-1} potassium nitrate) without added surfactant. Each data point is an average for three droplets from a single sample.

3 MSD of dodecane droplets

We measured the mean-square displacement (MSD) of droplet centroids over 60 s. Using Matlab, we detected the position of the oil-water interface for each droplet in an image and thereby located the droplet centroid. From the width of the oil-water interface, we estimated that the error on the position of the droplet centroid was 0.5 μm . Subsequently, we calculated the centroid MSD for three droplets of a given diameter (Fig. S6). Differences between MSDs for biological replicates reflect differences in the interaction of the droplets with the underlying glass substrate.

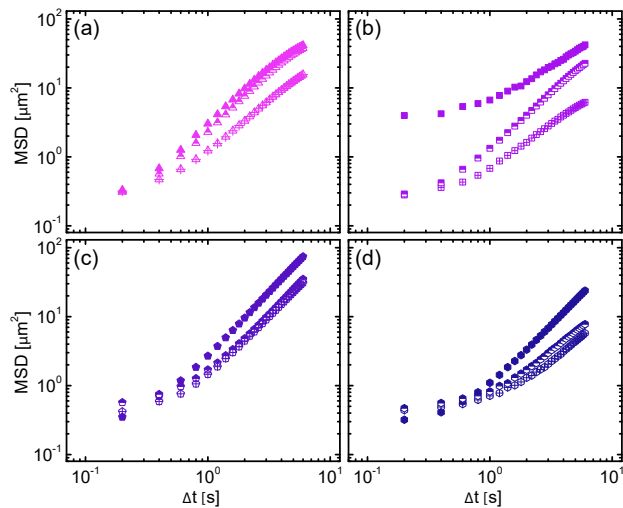


Fig. S5 Mean-square displacement (MSD) of the droplet centroid as a function of time for droplets of diameter (a) $30 \pm 1 \mu\text{m}$, (b) $40 \pm 1 \mu\text{m}$, (c) $60 \pm 1 \mu\text{m}$, and (d) $70 \pm 1 \mu\text{m}$.

The MSD for a fixed droplet diameter did not correlate with angular speed (Fig. S6a,b) or optical density (Fig. S6c). This is likely due to the surface heterogeneity in the glass capillaries, leading to pronounced variations in interactions of droplets with the surface.

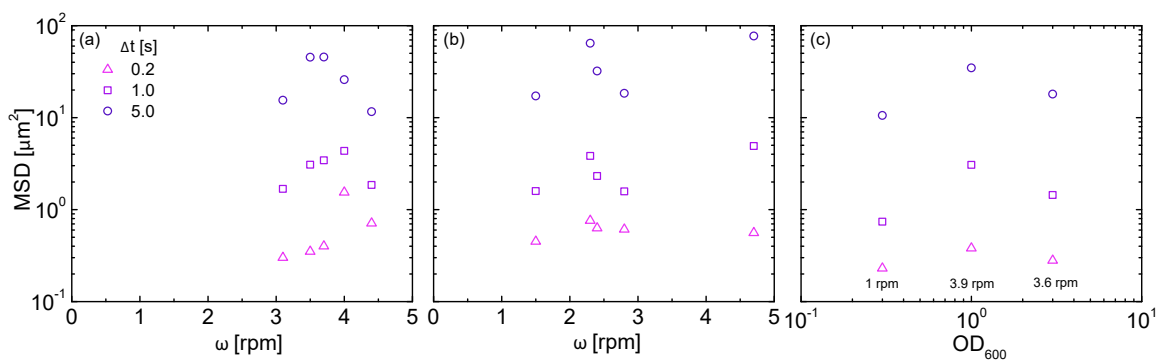


Fig. S6 Mean-square displacement (MSD) as a function of angular speed (a and b) and optical densities (c) for droplets of diameter (a) 40 μm , (b) 65 μm , and (c) 30 μm .

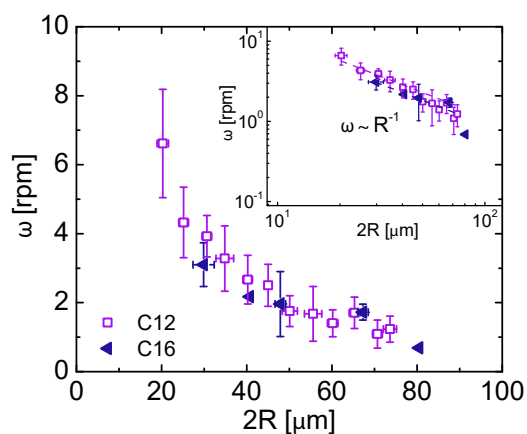


Fig. S7 Angular speed as a function of drop diameter for dodecane and hexadecane droplets. Optical density of *H. titanicae* suspension is 1.0. The aqueous phase is water (10 gL^{-1} potassium nitrate) with no added surfactant.

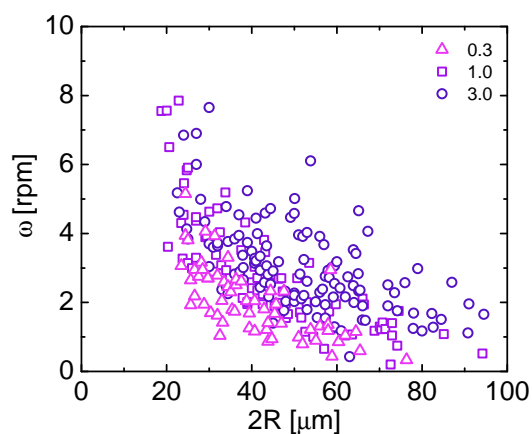


Fig. S8 Angular speed of dodecane droplets as a function of droplet diameter for OD of 0.3, 1.0, and 3.0. The aqueous phase is water (10 gL^{-1} potassium nitrate) with no added surfactant.

4 Model for droplet rotation

The torque due to rotational drag^{3,4} on a rotating droplet is given by $T_{\text{drag}} = 8\pi\mu R^3\omega$, where R is the radius of the droplet, μ is the suspension viscosity, and ω is the angular speed of the droplet. There is an additional drag on the droplet due to fluid flow generated by rotation of flagella. If we neglect this drag compared to the rotational drag then we can model the bacterium as a force monopole following Ref. 5. In this scenario the angular rotation of the droplets scales as R^{-1} with one fitting parameter (Fig. S9(a)). If instead the bacterium is treated as a force dipole, the drag force due to fluid flow is significant and the angular rotation of the droplets scales as $[1 - R(l^2 + R^2)^{-0.5}]/R$, where $l = 10 \mu\text{m}$ is the length of a flagellum and is held constant (Fig. S9(b)). The dashed lines in Fig. S9(a) indicate the fits to $\omega = \frac{F_a}{4\eta\sqrt{\pi A_0}} \frac{1}{R}$, and dashed lines in Fig. S9(b) indicate the fits to $\omega = \frac{F_a}{4\eta\sqrt{\pi A_0}} \frac{1}{R} [1 - R(l^2 + R^2)^{-0.5}]$, where $\frac{F_a}{4\eta\sqrt{\pi A_0}}$ is a fitting parameter in both panels and $l = 10 \mu\text{m}$ is a constant.

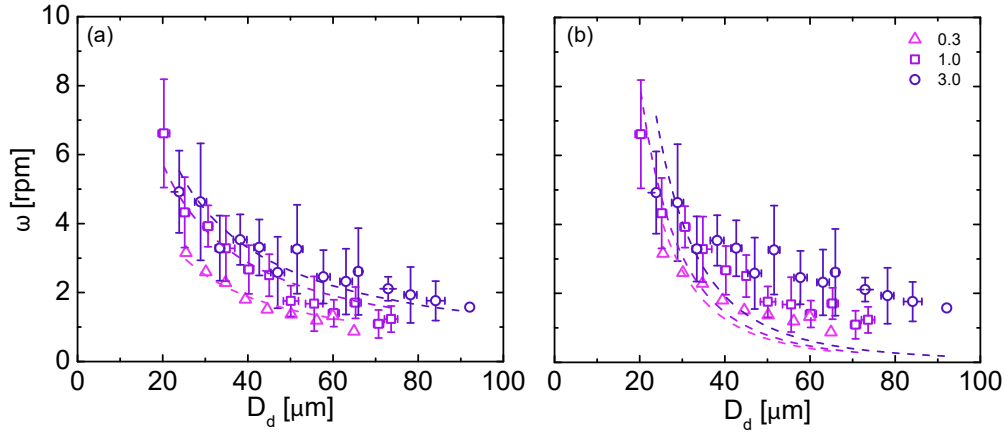


Fig. S9 Angular velocity as a function of droplet diameter with (a) monopole and (b) dipole model (Ref. 5).

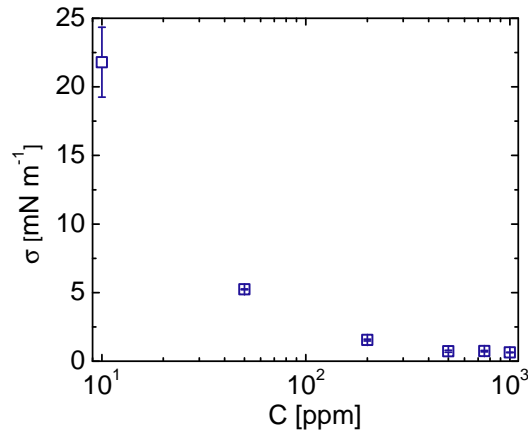


Fig. S10 Dodecane-water interfacial tension σ as a function of dioctyl sodium sulfosuccinate (DOSS) concentration. Water contains 10 gL^{-1} of potassium nitrate.

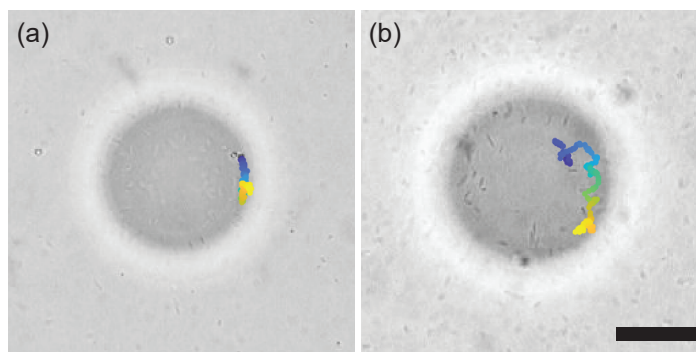


Fig. S11 PS particle trajectories on rotating droplets for *S. halotis* concentrations of (a) 2.7×10^9 cells mL^{-1} and (b) 8.7×10^9 cells mL^{-1} . Droplet in (a) rotated at 0.2 rpm whereas droplet in (b) rotated at 0.5 rpm. Scale bar is 20 μm .

References

- 1 S. Wu, *J. Adhes.*, 1973, **5**, 39–55.
- 2 S. Wu, *J. Polym. Sci. Part C: Polym. Symp.*, 1971, pp. 19–30.
- 3 H. Lamb, *Hydrodynamics*, Cambridge University Press, 6th edn., 1945.
- 4 S. Rubinow and J. B. Keller, *J. Fluid Mech.*, 1961, **11**, 447–459.
- 5 J. Schwarz-Linek, C. Valeriani, A. Cacciuto, M. Cates, D. Marenduzzo, A. Morozov and W. Poon, *Proc. Natl. Acad. Sci. USA*, 2012, **109**, 4052–4057.